

Muon spin rotation and SQUID investigation of superconductivity in $(\text{NH}_3)_x\text{NaK}_2\text{C}_{60}$ ($x \sim 0.7$)

M. Riccò,* T. Shiroka, E. Zannoni, F. Barbieri, and C. Bucci

Dipartimento di Fisica and Istituto Nazionale di Fisica della Materia, Università di Parma, Parco Area delle Scienze 7/a, 43100 Parma, Italy

F. Bolzoni

Istituto Maspec-CNR, Parco Area delle Scienze, Loc. Fontanini, 43010 Parma, Italy

(Received 28 May 2002; revised manuscript received 4 October 2002; published 31 January 2003)

The family of superconducting fullerides $(\text{NH}_3)_x\text{NaK}_2\text{C}_{60}$ shows an anomalous correlation between T_c and lattice parameter. To better understand the origin of this anomaly we have studied a representative $x=0.72$ compound using superconducting quantum interference device (SQUID) magnetometry and muon spin rotation spectroscopy. The lower critical field H_{c1} , measured by the trapped magnetization method, is less than 1 G, a very small value as compared with that of other fullerides. Muon spin depolarization in the superconducting phase shows also quite small local-field inhomogeneities, of the order of those arising from nuclear dipolar fields. On the other hand, the 40-T value for H_{c2} , as extracted from magnetometry data, is comparable to that of other fullerides. We show that these observations cannot be rationalized within the framework of the Ginzburg-Landau theory of superconductivity. Instead, the anomalous magnetic properties could be interpreted taking into account the role played by polaronic instabilities in this material.

DOI: 10.1103/PhysRevB.67.024519

PACS number(s): 74.70.Wz, 74.20.Mn, 76.75.+i

I. INTRODUCTION

In fullerene based superconductors ammonia intercalates as a neutral molecule, without interacting with the host electronic system and preserving the superconducting properties of the material. Since it acts simply as a molecular spacer, a change in lattice parameters and an increase of unit-cell volume are often observed.¹ As a consequence, the t_{1u} conduction band of the fullerene compound narrows and its density of states at the Fermi level increases, thus determining an increment in the superconducting transition temperature. An example of this mechanism has been reported for $\text{Na}_2\text{CsC}_{60}$,¹ which gives $(\text{NH}_3)_4\text{Na}_2\text{CsC}_{60}$ after ammoniation, with a conspicuous increase in transition temperature from 10.5 to 29.6 K.

The intercalation of ammonia can also induce a metal-to-insulator transition as, e.g., in $\text{NH}_3\text{K}_3\text{C}_{60}$,^{2,3} where the superconductivity of the ammoniated compound can be restored only after the application of external pressure.⁴

We will deal here with a family of fullerides such as $(\text{NH}_3)_x\text{NaK}_2\text{C}_{60}$ and $(\text{NH}_3)_x\text{NaRb}_2\text{C}_{60}$, whose precursors $\text{NaK}_2\text{C}_{60}$ and $\text{NaRb}_2\text{C}_{60}$ cannot exist as a single phase in normal conditions, but become stable only as ammoniated compounds.⁵ X-ray diffraction in these systems shows that the NH_3 -Na groups occupy the large octahedral sites⁵ with a consequent off-centering of the Na^+ ions. Since their discovery, these compounds have revealed puzzling features concerning the relation between the superconducting transition temperature both with the lattice parameter as well as with the density of states at the Fermi level. Indeed, the progressive removal of NH_3 , accomplished by pumping on the sample above room temperature, results in a *decrease* of the lattice parameters accompanied by an *increase* of the superconducting transition temperature, a trend opposite to that observed in $(\text{NH}_3)_4\text{Na}_2\text{CsC}_{60}$. In addition, we have recently shown⁶ that in a series of $(\text{NH}_3)_x\text{NaK}_2\text{C}_{60}$ compounds (with

$0.5 < x < 0.8$) the Pauli-Landau spin susceptibility yields a *lower* density of states at the Fermi level in compounds having a *higher* T_c , in contrast with BCS or Migdal-Eliashberg predictions.

It is therefore interesting to ask whether these anomalies are related to essential differences in the nature of superconductivity in $(\text{NH}_3)_{0.72}\text{NaK}_2\text{C}_{60}$ with respect to most common superconducting fullerides. A possible nonconventional nature of the superconductivity in this system would manifest itself in the values of the critical parameters of its superconducting phase: the London penetration depth λ and the lower and upper critical fields, H_{c1} and H_{c2} , respectively.

From the available data in the literature, the other so-called “normal” fullerene based superconductors appear to be extreme type-II superconductors^{7,8} characterized by $\kappa = \lambda/\xi \gg 1$, where κ is the Ginzburg-Landau parameter. Our results will be first analyzed in this framework and, in case of discrepancies, alternative suggestions will be offered.

When $\lambda \gg \xi$, both of these fundamental lengths can be easily extracted from measurements of the lower (H_{c1}) and the upper (H_{c2}) critical magnetic fields or, more precisely, from their extrapolated values at zero temperature. Roughly speaking, H_{c2} , the field at which the transition from the superconducting to the normal state occurs, corresponds to the field at which one quantum of magnetic flux $\Phi_0 = hc/2e \approx 2 \times 10^{-7}$ G cm² extends over the coherence area of an electron pair, so that

$$H_{c2}(0) = \frac{\Phi_0}{2\pi\xi^2}, \quad (1)$$

from which the Ginzburg-Landau coherence length ξ can be determined. On the other hand, the knowledge of H_{c1} , the field at which the magnetic flux starts to penetrate the sample, allows the computation of the penetration depth λ by using the well-known equation (valid for $\kappa \gg 1$)

$$H_{c1}(0) = \frac{\Phi_0}{4\pi\lambda^2} \ln \kappa. \quad (2)$$

In addition to independent measurements of H_{c1} and H_{c2} , as obtained by standard superconducting quantum interference device (SQUID) magnetometry, we will provide also the value for λ , which yields a stringent check of the validity of Eqs. (1) and (2). Since λ represents the transverse extension of the vortices in the Abrikosov intermediate phase, its value can be also determined from the local magnetic-field distribution. It is well known that muon spin rotation (μ SR) gives reasonable estimates of λ , even for irregular flux-line lattices. Details on SQUID and μ SR measurements are given in the next section.

II. EXPERIMENT

The samples were prepared following the procedures outlined in Ref. 5. Stoichiometric amounts of alkali metals (Aldrich, 99.95%) and C_{60} (Southern Chem. 99.5%) were dissolved in anhydrous ammonia (Aldrich, 99.99+%) at 230 K. After the reaction had taken place, the temperature was slowly increased until the ammonia was completely evaporated. The successive pumping at 120 °C for 30 min yielded the compound $(NH_3)_{0.72}NaK_2C_{60}$; the sample was then annealed at 100 °C for 10 days. Its transition temperature was $T_c = 12$ K and it showed a 20% superconducting fraction, indicative of bulk superconductivity in its powder form. The ammonia concentration $x = 0.72$, as determined from 1H NMR measurements, is in good agreement with the concentration extracted from an interpolation of the $T_c - x$ data reported in Ref. 5. Evaluation of the granulometry of the samples was performed using a scanning electron microscope (SEM), whose micrographs indicate an average particle size $d \sim 2 \mu m$.

dc magnetometry measurements were performed with a Quantum Design SQUID magnetometer equipped with a home built Helmholtz cube which surrounded the whole instrument body, thus allowing a reduction of the residual field on the sample to less than 2 mG. The SQUID superconducting magnet was cooled from RT to liquid-He temperature in zero external field. For a good thermal contact even at low temperatures the sample was sealed in a long quartz tube under 1 mbar of He atmosphere. The sample was suspended in the middle of the tube, whose length was chosen so as to always have a tube portion face the SQUID coils, even when the sample had to move in and out of them during the magnetic moment measurement. This expedient allowed an accurate subtraction of the quartz diamagnetic contribution.

μ SR, which measures the spin precession of implanted muons, is very sensitive to local magnetic fields and therefore it constitutes a valuable technique for our purposes. Indeed, when the applied transverse field exceeds H_{c1} , the field distribution of the flux-line lattice will damp the muon spin precession signal, hence the penetration depth can be readily extracted⁹ from the damping rate.

In common metals and superconductors all the implanted muons usually sit interstitially and, being screened by con-

duction electrons, they will not form any paramagnetic bound state (muonium). Hence their precession frequency in an external magnetic field remains that of a free particle (diamagnetic muon). In C_{60} based superconductors, besides this major component there is an additional part of implanted muons (typically 10–20%) which will form endohedral muonium (located inside a C_{60} molecule), whose precession frequency is much higher than that of diamagnetic muon. Here we are interested only in the majority of muons that come at rest in the fcc lattice interstices (the precise location is not well known) and precess as diamagnetic muons, i.e., with a gyromagnetic ratio $\gamma_\mu = 13.55$ kHz/G.

When a superconductor is in the intermediate state, i.e., $\mu_0 H_{c1} < B < \mu_0 H_{c2}$, the muon precession signal will be damped by the inhomogeneous magnetic-field distribution of the vortices. The expected damping profile (or the corresponding line shape in Fourier space) in the case of a triangular flux-line lattice has been computed¹⁰ and, for single crystals, also successfully measured. Unlike single crystals, polycrystalline or powder materials exhibit a smeared out magnetic-field distribution, with the consequence that the μ SR line will assume a Gaussian shape ($\sigma_{sc} \sim 0.1 - 0.6 \mu s^{-1}$ for fullerides) below T_c .⁹ The established relation between the μ SR damping rate $\sigma_{sc}(0)$ and the internal field rms deviation ΔB is given by $\Delta B = \sigma_{sc}(0)/2\pi\gamma_\mu$. Once ΔB is known from an experiment that measures $\sigma_{sc}(0)$ in the appropriate intermediate field range $\mu_0 H_{c1} < B < \mu_0 H_{c2}$, the penetration depth λ is given by¹⁰

$$\lambda \approx 3.71 \times 10^{-3} \cdot \left[\frac{\Phi_0^2}{(\Delta B)^2} \right]^{1/4}. \quad (3)$$

μ SR experiments were performed on the EMU spectrometer of the ISIS Facility (Rutherford Laboratory, UK). The pulsed nature of the muon beam sets an upper frequency cutoff that prevents the direct observation of high muonium frequencies. Nevertheless, the interesting fraction of diamagnetic muons will precess well within the pass band of the spectrometer and therefore could be readily measured. In our case, the sample (~ 500 mg) was pressed inside an air tight aluminum cell equipped with a thin ($75\text{-}\mu m$) Kapton window. A pure silver foil was put both directly behind the sample and around the cell window to make it easy to subtract the signal coming from the sample holder.

III. SQUID MEASUREMENTS

A. Lower critical field

In spite of many previous measurements of the lower critical field by SQUID magnetometry in fullerides,^{7,8,11–18} its precise determination is still controversial due to considerable experimental difficulties. The simplest way to measure H_{c1} consists in observing the field at which the $M = M(H)$ curve starts to deviate from linearity. Unfortunately data on fullerides never show a good linearity and this brings to an overestimate of the H_{c1} value. Alternative methods based on Bean's critical state model¹⁹ give quite different values.¹⁴ Recently it was shown¹⁶ that the measurement of the trapped

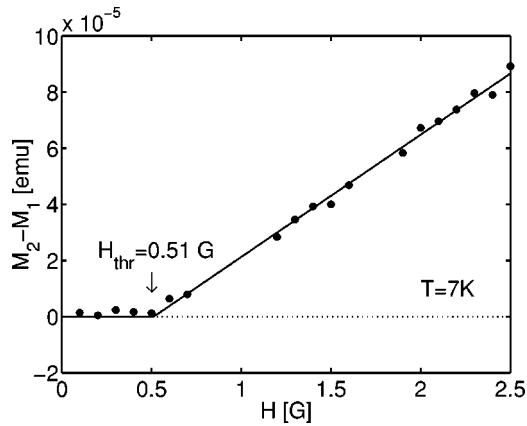


FIG. 1. The trapped magnetization $M_2 - M_1$ as a function of the applied field H in $(\text{NH}_3)_{0.72}\text{NaK}_2\text{C}_{60}$. The lower critical field H_{c1} is determined from the onset of the magnetization which starts is trapped at $H = H_{\text{thr}}$.

magnetization in the intermediate phase yields a more reliable determination of H_{c1} . The procedure is as follows: first the sample is cooled in zero field from above T_c and its initial magnetic moment (M_1) is measured (ideally it should be zero, but a residue always exists). Then a magnetic field H is applied for at least 30 s and, after switching it off, the final moment (M_2) is measured. When the applied field exceeds a threshold value H_{thr} the magnetic flux is trapped inside the sample. This trapped magnetization, given by the difference $M_2 - M_1$, is then plotted against the applied field H , as shown in Fig. 1 for measurements on $(\text{NH}_3)_{0.72}\text{NaK}_2\text{C}_{60}$ performed at 7 K. The increase of the trapped magnetization above H_{thr} , which follows a linear behavior at all the investigated temperatures, allows a much more precise determination of H_{c1} than alternative procedures. The fitted value for trapping onset (0.51 G for the linear fit shown in Fig. 1) is related to the lower critical field value by $H_{c1} = H_{\text{thr}} / (1 - n)$, where n is the demagnetization factor. Preliminary measurements on powdered samples gave essentially the same results, although the trapped magnetization values were rather scattered around the (same) fit line (see Fig. 1). The use of (weakly compressed) pellets remarkably reduced the spread without an appreciable change in H_{thr} , confirming that the demagnetization factor of a set of independent spheres ($n = 1/3$), correctly adopted for powders,¹⁶ is appropriate also for pellets.

The results of several H_{c1} measurements at different temperatures are illustrated in Fig. 2. The zero-temperature value $H_{c1}(0) = 0.87$ G was then extrapolated from a parabolic fit (BCS weak coupling gave a similar result and experimental errors do not allow us to distinguish between the different behaviors).

The striking feature about the $H_{c1}(0)$ is its low value with respect to that of other fullerides, shown in Table I for a comparison. Even an unphysical linear fit of the data would at most yield an extrapolated value $H_{c1}(0) \sim 1.2$ which still is one order of magnitude smaller than $H_{c1}(0)$ for the quoted fullerides. The obvious suspicion that the powdered nature of the sample affects the measured values was addressed in a previous experiment, reported in Ref. 16, where a powdered

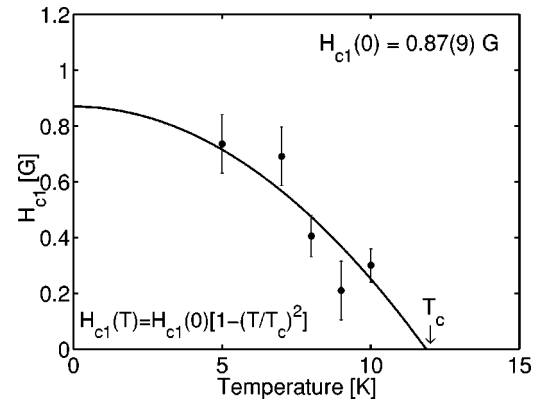


FIG. 2. Measured H_{c1} values as a function of temperature. The extrapolation of the parabolic fit at $T=0$ yields $H_{c1}(0) = 0.87(9)$ G.

$\text{RbCs}_2\text{C}_{60}$ sample and a single crystal were compared and found to have the same lower critical field value. Hence the measured low H_{c1} value given here will be considered an intrinsic feature of the compound.

B. Upper critical field

The upper critical field H_{c2} can be determined from the temperature dependence of the field-cooled magnetization.¹⁴ In this case the sample is cooled in an externally applied field H ($0.5 < H < 5.5$ T) starting from $T > T_c$ and its magnetic moment is measured. The value of the external field corresponds to H_{c2} when the temperature equals the relative T_c . Figure 3 shows an example of such a measurement in a 3-T magnetic field.

The data above T_c were fitted to a Curie behavior coming from paramagnetic impurities, to which one must add a temperature-independent component resulting from Pauli, Landau, and core contributions to susceptibility (upper part of the figure).⁶ After subtraction of all these contributions the curve shown in the lower part of Fig. 3 is obtained. T_c was estimated as the temperature at which the linear interpolation of the data in the superconducting state intersects the normal-state baseline. The observed superconducting transition temperature $T_c(H)$ decreases on increasing H_{appl} . In Fig. 4 we report the dependence of the critical temperature on H_{appl} . Unfortunately, the maximum field available in our conventional SQUID magnetometer ($H_{\text{max}} = 5.5$ T) does not allow us to investigate the full range of $T_c = T_c(H_{\text{appl}})$ dependence

TABLE I. Comparison of lower critical fields H_{c1} for several alkali-metal-doped fullerides (powders denoted by asterisk).

Compound	$H_{c1}(T=0)$ [G]	Ref.
Rb_3C_{60}	~ 50	13
Rb_3C_{60}	13*	16
$\text{RbCs}_2\text{C}_{60}$	~ 80	14
$\text{RbCs}_2\text{C}_{60}$	16*	16
K_3C_{60}	12*	16
$(\text{NH}_3)_{0.72}\text{NaK}_2\text{C}_{60}$	0.87(9)*	this work

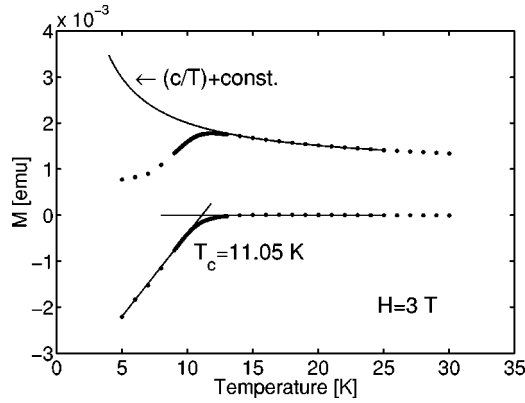


FIG. 3. Upper graph: Field-cooled magnetization of $(\text{NH}_3)_{0.72}\text{NaK}_2\text{C}_{60}$ at $H=3$ T: the fitted curve accounts for paramagnetic impurities and Pauli contributions. Lower graph: After the subtraction of the above-mentioned contributions, T_c , at $H_{\text{appl}} = H_{c2}$, is determined from the intersection of the two linear fits.

so that we have to resort to extrapolation. The extrapolated field value at zero temperature (relevant for ξ calculation) is usually extracted from the slope of the observed linear behavior using the Werthamer-Helfand-Hohenberg (WHH) formula:²⁰

$$H_{c2}(0) = 0.69 T_c \cdot \left. \frac{\partial H_{c2}}{\partial T} \right|_{T=T_c}. \quad (4)$$

The value for the derivative is 5.0 ± 0.3 T/K and from Eq. (4) we find $H_{c2}(0) = 40 \pm 2$ T. If we use Eq. (1), we can extract a coherence length $\xi = 2.86(8)$ nm. Both of these values, although different, do not appear to be inconsistent with those of other C_{60} based superconductors.²¹

Similarly to the measurement of H_{c1} it is important to examine possible factors that could affect the estimated value for H_{c2} :

(i) According to analogous measurements on K_3C_{60} ,²² the parabolic $H_{c2}(T)$ dependence predicted by the WHH theory²⁰ was not observed: the use of such theory to extract $H_{c2}(0)$ was shown to produce an underestimated value. By

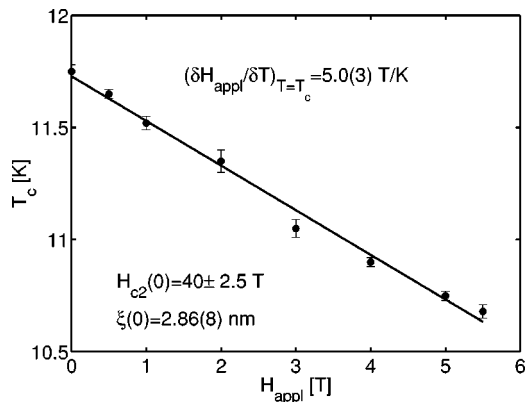


FIG. 4. Critical temperature dependence on H_{appl} . The upper critical field $H_{c2}(0) = 40 \pm 2.5$ T is found from the extrapolated slope $\partial H_{\text{appl}} / \partial T_c$ using formula (4).

guessing from Ref. 22 a plausible enhancement factor of 2 in our data, we point out that Eq. (1) would predict a still smaller ξ (~ 2 nm), which has an important role in the discussion that will follow.

(ii) It is known that sample granularity enhances the measured $H_{c2}(0)$ values due to the onset of zero-dimensional (0-D) fluctuations, as detected in conductivity measurements in K_3C_{60} .²³ This effect is expected to become dramatic when the grain size d becomes comparable to ξ . Indeed, also conventional superconductors like Al, in a suitable fine granular form, can have an upper critical field nearly two orders of magnitude larger than that of bulk samples.²⁴ The granularity of the material we have investigated, however, involves an average particle size of ~ 2 μm , which is more than three orders of magnitude larger than any estimate for ξ , thus allowing us to definitely exclude any appreciable H_{c2} enhancement effect due to granularity.

In conclusion we can state that the coherence length we find from H_{c2} measurements is accurate and, due to its inverse square-root dependence from H_{c2} , even large uncertainties in the determination of the latter would not appreciably affect the ξ value.

IV. MUON SPIN ROTATION MEASUREMENTS

As briefly described in Sec. II, μSR damping rate measurements yield a reasonable value for the penetration depth λ , even for an irregular flux-line configuration, typical for powders or polycrystalline samples. In our experiment the sample was field cooled in an external transverse field of 50 G from above T_c and the muon precession histograms measured at fixed T . The presence of two precessing signals at all temperatures indicated that a fraction of the total muons came at rest in the sample holder while the other in the sample. The two components could be easily singled out thanks to their differences not only in amplitude, but mainly in their precession frequency (diamagnetic shift due to superconducting material) and damping rate (internal field second moment due to flux-line lattice). In accounting for the whole expected signal, a missing fraction was detected: it is well known that this fraction is entirely due to the formation of endohedral muonium—i.e., muonium atoms at rest within the C_{60} cage—while the formation of muonium adduct radicals is inhibited in C_{60}^{n-} compounds. This fraction is “missing” because, at the applied field of 50 G, its characteristic frequency is too high to be observable at the ISIS facility. In passing, it must be pointed out that this missing muonium fraction is not interesting for the present experiment, where we look for the information yielded by the unbound muons in the material’s interstitial sites.

The signal due to the sample shows a Gaussian decay with a decay rate σ , which was fitted using the function $\sin(\omega t + \phi) \exp(-\sigma^2 t^2 / 2)$. Figure 5 shows the fitted values for σ in the temperature range $4 < T < 15$ K. The temperature-independent residual value as observed above T_c is due to the magnetic-field distribution of the randomly oriented nuclear dipoles (^1H , ^{14}N , ^{23}Na , $^{39,40,41}\text{K}$, ^{13}C).

The additional broadening below T_c , due to the flux-line lattice formation, is smaller than the nuclear term and much smaller than that found in similar fullerenes such as Rb_3C_{60}

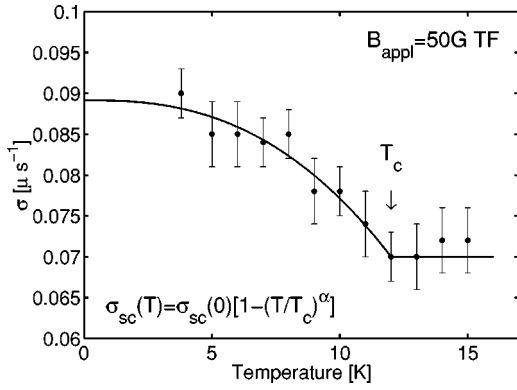


FIG. 5. μ SR Gaussian decay rate as a function of temperature in a 50-G transverse field. The fit of data below T_c yields σ_{sc} , from which the field distribution inside the sample is found. The penetration depth λ is then calculated using Eq. (3).

and K_3C_{60} .⁹ The superconducting contribution and the normal-state nuclear dipole broadening add in quadrature, hence the former (σ_{sc}) can be extracted. The temperature dependence of σ_{sc} was fitted to the phenomenological temperature dependence: $\sigma_{sc}(T) = \sigma_{sc}(0)[1 - (T/T_c)^\alpha]$, which yields $\sigma_{sc}(0) = 5.5 \times 10^{-2} \mu s^{-1}$ and $\alpha = 2.55$. The same experiment was repeated applying a 100-G transverse field and a similar σ_{sc} value to that of the 50-G case was found, typical of systems with $\lambda \gg \xi$.¹⁰ The value for the London penetration depth λ can be extracted from Eq. (3) which gives $\lambda = 1.40 \mu m$. This value is more than two times larger than that of other superconducting fullerenes. In thinking of effects that could enhance the measured λ a possible candidate is the granulometry of the sample, when the particle size is not much larger than λ .³³ But this is just our case, where being $d \sim \lambda$, we do expect strong surface effects which tend to increase the measured λ value with respect to that of a bulk sample. Although we have no means to implement a quantitative correction to the measured value, we can definitely state that it represents an upper limit for the real penetration depth, which certainly cannot be larger than $1.4 \mu m$.

V. DISCUSSION

In the previous section we described the independent measurements of H_{c1} , H_{c2} , and λ and anticipated that they would be used within the framework of the Ginzburg-Landau-Abrikosov equations (1) and (2). In principle, the knowledge of H_{c1} and H_{c2} values is sufficient to extract the coherence length ξ and the penetration depth λ . The additional experimental value of λ from μ SR measurements helps in checking the internal consistency. From Eq. (1) the experimental value of $H_{c2} = 40$ T yields $\xi = 2.86(8)$ nm; with this value and the experimental result for $H_{c1} = 0.87$ G Eq. (2) yields $\lambda = 3.82 \mu m$. If only H_{c1} and H_{c2} were measured, the values for ξ and λ (although the latter seems considerably larger than the value found in other superconducting fullerenes) would appear acceptable for an extreme type-II superconductor.

The picture appears inconsistent, however, since we must account for the *measured* value of $\lambda = 1.4 \mu m$, which is

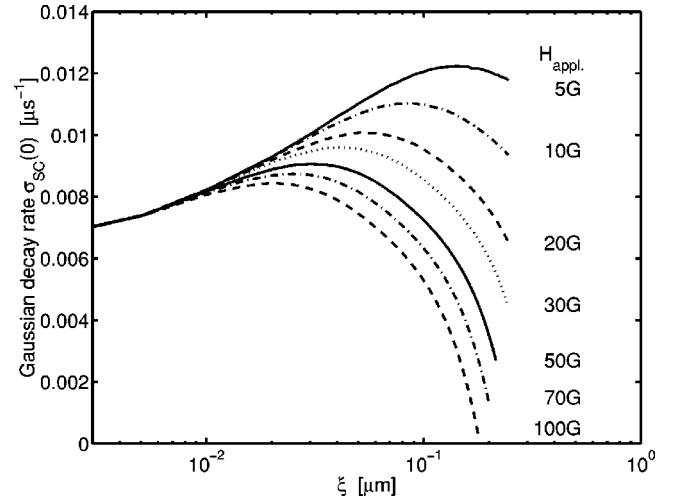


FIG. 6. μ SR signal decay rate σ_{sc} as a function of coherence length ξ as obtained from the numerical solution of the GL equations. The different curves correspond to several values of applied magnetic field; the lower critical field value was fixed at $H_{c1} = 0.87$ G.

nearly three times smaller than that predicted by Eqs. (1) and (2). Such a discrepancy is by no means trivial because, in order to weaken it, one has to make unphysical assumptions on the other measured parameters, i.e., the two critical fields. Indeed, as can be seen from Eqs. (1) and (2), even quite a small variation in λ will determine orders of magnitude variations in the critical fields.

As an additional check for the observed discrepancy we have also used some approximate analytical solutions of the Ginzburg-Landau (GL) equations. Specifically, we compute the muon spin depolarization rate σ_{sc} , which can easily be compared with the experimental value. The calculation requires a numerical solution of the GL equations which was performed using the efficient algorithm developed in Ref. 25. This fast iterative variational procedure, which minimizes the free-energy density f , gives as an output the local magnetic-field distribution $B = B(x, y)$. The second moment of the local fields ΔB yields the damping rate (σ_{sc}) of the μ SR.

The results of this calculation are shown in Fig. 6 which reports the dependence of σ_{sc} on the coherence length ξ as predicted by the GL equations for a fixed $H_{c1} = 0.87$ G. The different curves refer to different values of the applied field in the range $5 < B < 100$ G. It appears evident that the maximum predicted value for the muon decay rate at the applied field of 50 G is $9 \times 10^{-3} \mu s^{-1}$, much smaller than the measured value of $55 \times 10^{-3} \mu s^{-1}$ and, in any case, too small to be measured. This confirms that the H_{c1} , H_{c2} , and λ values measured in $(NH_3)_{0.72}NaK_2C_{60}$ cannot be representative of a superconducting system described by the Ginzburg-Landau theory. In addition, the fact that a series of samples with different ammonia content have critical temperatures inversely proportional to the density of states at the Fermi level, as recalled in the Introduction, is consistent with this conclusion.

Even though the phonon-mediated superconductivity in

fullerides is well established, we suggest that polaron-based theories of superconductivity can correctly describe some of these systems, such as those considered in this work. Unlike the BCS or Migdal-Eliashberg alternatives, the polaronic approach does not require the phonon energy scale to be much smaller than that of electrons. In fullerides, indeed, typical phonon energies involved in the superconducting coupling are of the order of 0.15 eV, due to the intramolecular H_g modes of C_{60} .²⁶ According to the early predictions of Bulaevskii *et al.*²⁷ for the superconducting properties of systems with local pairs, critical fields and critical length values are expected to be significantly different from those of ordinary BCS superconductors; in particular, the lower critical field H_{c1} is expected to be much smaller and the penetration depth λ much larger than the respective BCS counterparts. More recently, a polaron-based analysis has been formulated, with the inclusion of nonadiabatic effects in the Migdal-Eliashberg theory, in order to better predict transition temperatures and photoelectron spectra of fullerides.²⁸ The presence of charge instabilities or fluctuations (charge disproportion, charge-density waves, etc.) predicted in polaronic systems manifests itself, indirectly, in superconducting fullerides in the following circumstances: (i) the NMR detection of a spin gap in the Na_2CsC_{60} superconductor as due to the presence of Jahn-Teller distorted $C_{60}^{(2,4)-}$ originating from a dynamic charge disproportion;²⁹ and (ii) the existence of a nonmagnetic insulating phase in $(NH_3)_2NaK_2C_{60}$,³⁰ interpreted in terms of a possible (dynamic) charge disproportion. Polaronic instabilities are in general expected at high values of the electron-phonon coupling constant ($\lambda_c \sim 1.5-2$).³¹ In the case of fullerides, though, the coupling values suggested by different experimental techniques (even though still under debate³²) settle in

a $0.5 < \lambda_c < 1.2$ range. The closeness of the upper limit of this range to that of the previously mentioned polaronic superconductivity boundary could suggest a possible role played by polarons in these systems.

VI. CONCLUSIONS

In this work we have shown that the magnetic properties of the fullerene based superconductor $(NH_3)_{0.72}NaK_2C_{60}$ are quite different from those of other fullerides, namely it displays a very small H_{c1} associated with very large H_{c2} and λ values. These results cannot be explained within the framework of the Ginzburg-Landau (GL) theory. It is suggested that the system considered here represents a borderline case, in which the nature of superconducting coupling begins to switch from a phonon-mediated to a polaronic character.

Indeed, electron-phonon interaction could be sufficiently large in general to make it possible for some systems, like $(NH_3)_xNaK_2C_{60}$, to exhibit an enhancement of the coupling which, in turn, favors the development of polaronic instabilities. In the present situation, specific quantitative predictions for measurable superconducting quantities are needed in order to understand the experimental results and clarify the essential nature of superconductivity in fullerides.

ACKNOWLEDGMENTS

We thank Professor E. H. Brandt who kindly provided us with the simulation code for muon spin depolarization calculations and Dr. G. Salvati with Dr. N. Armani who performed the SEM granulometry measurements. We acknowledge financial support by the EU Improvement of Human Potential (IHP) program, which sponsored part of our μ SR experiments at ISIS facility (UK).

*Electronic address: Mauro.Ricco@fis.unipr.it; URL: <http://www.fis.unipr.it/~ricco/>

- ¹O. Zhou, R.M. Fleming, D.W. Murphy, M.J. Rosseinsky, A.P. Ramirez, R.B. van Dover, and R.C. Haddon, *Nature* (London) **362**, 433 (1993).
- ²Y. Iwasa, H. Shimoda, T.T.M. Palstra, Y. Maniwa, O. Zhou, and T. Mitani, *Phys. Rev. B* **53**, R8836 (1996).
- ³H. Kitano, R. Matsuo, K. Miwa, A. Maeda, T. Takenobu, Y. Iwasa, and T. Mitani, *Phys. Rev. Lett.* **88**, 096401 (2002).
- ⁴O. Zhou, T.T.M. Palstra, Y. Iwasa, R.M. Fleming, A.F. Hebard, P.E. Sulewski, D.W. Murphy, and B.R. Zegarski, *Phys. Rev. B* **52**, 483 (1995).
- ⁵H. Shimoda, Y. Iwasa, Y. Miyamoto, Y. Maniwa, and T. Mitani, *Phys. Rev. B* **54**, R15 653 (1996).
- ⁶M. Riccò, T. Shiroka, A. Sartori, F. Bolzoni, and M. Tomaselli, *Europhys. Lett.* **53**, 762 (2001).
- ⁷K. Holczer, O. Klein, G. Grüner, J.D. Thompson, F. Diederich, and R.L. Whetten, *Phys. Rev. Lett.* **67**, 271 (1991).
- ⁸G. Sparn, J.D. Thompson, R.L. Whetten, S. Huang, R.B. Kaner, F. Diederich, G. Grüner, and K. Holczer, *Phys. Rev. Lett.* **68**, 1228 (1992).
- ⁹W.A. MacFarlane, R.F. Kiefl, S. Dunsiger, J.E. Sonier, J. Chakalian, J.E. Fischer, T. Yildirim, and K.H. Chow, *Phys. Rev. B* **58**, 1004 (1998).

¹⁰E.H. Brandt, *Phys. Rev. B* **37**, 2349 (1988).

- ¹¹C. Politis, A.I. Sokolov, and V. Buntar, *Mod. Phys. Lett. B* **6**, 351 (1992).
- ¹²C. Politis, V. Buntar, W. Krauss, and A. Gurevich, *Europhys. Lett.* **17**, 175 (1992).
- ¹³V. Buntar, U. Eckern, and C. Politis, *Mod. Phys. Lett. B* **6**, 1037 (1992).
- ¹⁴V. Buntar, M. Riccò, L. Cristofolini, H.W. Weber, and F. Bolzoni, *Phys. Rev. B* **52**, 4432 (1995).
- ¹⁵V. Buntar, in *Proceedings of Fullerenes: Chemistry, Physics and New Directions*, edited by R. S. Ruoff and K. M. Kadish (Electrochemical Society, Reno, NV, 1995), Vol. VII, pp. 994–1008.
- ¹⁶V. Buntar, F.M. Sauerzopf, and H.W. Weber, *Phys. Rev. B* **54**, R9651 (1996).
- ¹⁷V.A. Buntar, F.M. Sauerzopf, H.W. Weber, A.G. Buntar, H. Kumani, and M. Haluska, *Low Temp. Phys.* **23**, 267 (1997).
- ¹⁸V. Buntar, C. Krutzler, W. Haluska, F. M. Sauerzopf, H. W. Weber, and H. Kuzmany, in *Proceedings of the Symposium on Recent Advances in the Chemistry and Physics of Fullerenes and Related Materials*, edited by K. M. Kadish and R. S. Ruoff (Electrochemical Society, San Diego, CA, 1998), Vol. 6, pp. 460–468.
- ¹⁹C.P. Bean, *Phys. Rev. Lett.* **8**, 250 (1962).
- ²⁰N.R. Werthamer, E. Helfand, and P.C. Hohenberg, *Phys. Rev.* **147**, 295 (1966).

- ²¹M. Baenitz, M. Heinze, K. Luders, I. Werner, and R. Schlogl, in *Physics and Chemistry of Fullerenes and Derivatives. Proceedings of the International Winterschool on Electronic Properties of Novel Materials*, edited by H. Kuzmany, J. Fink, M. Mehring, and S. Roth (World Scientific, Singapore, 1995), pp. 436–439.
- ²²G.S. Boebinger, T.T.M. Palstra, A. Passner, M.J. Rosseinsky, D.W. Murphy, and I.I. Mazin, *Phys. Rev. B* **46**, 5876 (1988).
- ²³J.G. Hou, X.D. Xiang, M.L. Cohen, and A. Zettl, *Physica C* **232**, 22 (1994).
- ²⁴A. Abeles, R.W. Cohen, and W.R. Stowell, *Phys. Rev. Lett.* **18**, 902 (1967).
- ²⁵E.H. Brandt, *Phys. Rev. Lett.* **78**, 2208 (1997).
- ²⁶O. Gunnarsson, *Rev. Mod. Phys.* **69**, 575 (1997).
- ²⁷L.N. Bulaevskii, A.A. Sobyenin, and D.I. Khomskii, *Zh. Eksp. Teor. Fiz.* **87**, 1490 (1984) [*Sov. Phys. JETP* **60**, 856 (1984)].
- ²⁸A.S. Alexandrov and V.V. Kabanov, *Phys. Rev. B* **54**, 3655 (1996).
- ²⁹V. Brouet, H. Alloul, T.-N. Le, S. Garaj, and L. Forró, *Phys. Rev. Lett.* **86**, 4680 (2000).
- ³⁰M. Riccò, G. Fumera, T. Shiroka, E. Zannoni, and F. Bolzoni (unpublished).
- ³¹P. Paci, E. Cappelluti, C. Grimaldi, and L. Pietronero, *Phys. Rev. B* **65**, 012512 (2002).
- ³²O. Gunnarsson and J.E. Han, in *Electronic Properties of Molecular Nanostructures. XV International Winterschool*, edited by H. Kuzmany, J. Fink, M. Mehring, and S. Roth, AIP Conf. Proc. No. 591 (AIP, Melville, NY, 2001), pp. 425–429.
- ³³In this case the profile of field distribution inside the grains has a reduced modulation due to the proximity of the grain walls, resulting in an apparently higher λ value.